

Casimir interactions as a probe of broadband optical response

Calum F. Shelden¹ and Jeremy N. Munday^{1*}

¹Department of Electrical and Computer Engineering, University of California, Davis, One Shields Avenue, Davis, CA 95616-5270, USA.
*email: jnmunday@ucdavis.edu

Abstract:

Casimir forces arise from quantum electromagnetic fluctuations and depend on the dielectric response of interacting materials across the entire frequency spectrum. Although this dependence is central to Lifshitz theory of the Casimir effect, the formulation of the force in terms of dielectric functions evaluated at imaginary frequencies has largely obscured its connection to real-frequency optical properties, limiting the use of Casimir interactions as a probe of materials. Here we demonstrate that Casimir force measurements encode sufficient information to reconstruct a material's broadband optical response. Using supervised machine learning to invert Lifshitz theory, we determine the complex permittivity of a material over more than seven orders of magnitude in frequency from a single force–distance curve. We show that measurements at different separations selectively constrain distinct frequency ranges of the dielectric response, providing direct physical insight into how quantum fluctuations sample the electromagnetic spectrum. These results establish Casimir interactions as a physically constrained, broadband spectroscopic tool and open new opportunities for optical characterization in regimes inaccessible to conventional techniques.

Introduction

Quantum and thermal fluctuations of the electromagnetic field give rise to dispersion forces between neutral objects, including van der Waals and Casimir interactions [1,4]. These forces emerge from how materials modify the spectrum of electromagnetic fluctuations through their frequency-dependent dielectric response and boundary conditions. As a result, Casimir interactions are not governed by a single resonant mode but instead reflect the collective contribution of electromagnetic fluctuations spanning the entire spectrum, from static fields to optical and ultraviolet frequencies [5–7]. This global sensitivity underlies the rich material dependence of Casimir forces and has enabled a wide range of phenomena, including tunable attraction and repulsion [8–13], anisotropy-induced torques [14–18], and self-assembly [19–22].

The theoretical description of Casimir forces between real materials is most naturally expressed within Lifshitz theory [2,3], in which material properties enter through the dielectric function evaluated at imaginary frequencies. This formulation arises from a contour transformation that simplifies the treatment of quantum fluctuations but obscures their connection to the real-frequency optical response typically measured in experiments [23,24]. Consequently, although Casimir forces are fundamentally determined by a material's broadband electromagnetic

properties, they have rarely been viewed as a practical probe of those properties. Instead, simulations and interpretations of Casimir interactions commonly rely on concatenated optical data sets, model extrapolations, or simplified oscillator descriptions, each of which introduces uncertainty and limits predictive accuracy [25–27].

The intrinsic broadband nature of Casimir forces nevertheless raises a fundamental question: *does a Casimir force measurement contain enough information to reconstruct a material's optical response?* In principle, the force integrates contributions from fluctuations across the electromagnetic spectrum, with different separation distances weighting different frequency ranges. In practice, however, analytically inverting Lifshitz theory to recover a material's permittivity from force data is intractable, and no general experimental approach for such an inversion has previously been demonstrated. Establishing whether and how this inversion can be achieved would transform Casimir interactions from a phenomenon that depends on optical properties into a tool for their determination.

Here we demonstrate a general approach for reconstructing a material's broadband dielectric response directly from Casimir force measurements. We generate physically motivated dielectric spectra, compute their corresponding Casimir interactions using Lifshitz theory, and train supervised machine-learning models to learn the inverse mapping between force–distance curves and complex permittivity. Using this framework, we reconstruct the real and imaginary components of a material's permittivity over more than seven orders of magnitude in frequency from a single Casimir force curve. We show that force measurements at larger separations preferentially constrain the low-frequency dielectric response, whereas measurements at shorter separations encode higher-frequency behavior, providing direct physical insight into how quantum fluctuations sample different spectral regimes. Finally, we apply this approach to experimentally measured Casimir force gradients, highlighting both the potential and current limitations of quantum-fluctuation-based optical characterization.

Results and Discussion

To determine whether Casimir force measurements encode sufficient information to reconstruct a material's broadband dielectric response, we treat the inversion of Lifshitz theory as a supervised learning problem [28–30]. We consider the Casimir interaction between a gold sensing surface and a planar sample with unknown optical properties, using the measured or simulated force as a function of separation as the sole input. The output of the model is the complex permittivity of the sample over a wide range of electromagnetic frequencies. Training data are generated by constructing physically motivated dielectric spectra and computing their corresponding Casimir forces using Lifshitz theory, thereby embedding the known physics of quantum fluctuation–induced interactions directly into the learning process. This framework allows us to assess both the fidelity with which broadband optical response can be reconstructed from force data and the physical origins of any limitations in that reconstruction.

Figure 1 illustrates the conceptual framework underlying the inversion of Casimir force measurements into broadband optical response. We consider the Casimir interaction between a gold sensing surface and a planar sample with unknown dielectric properties, using the measured

force as a function of separation as the only experimental input (Fig. 1a). Within Lifshitz theory, this force depends on the material’s dielectric response across the electromagnetic spectrum, with different separation distances weighting different frequency ranges. Our approach exploits this structured dependence by training supervised learning models to map force–distance curves onto the real and imaginary components of the sample’s permittivity over a wide frequency range (Fig. 1b). Rather than relying on an assumed analytical inversion, the model learns the nontrivial relationship between broadband quantum fluctuations and real-frequency optical response implied by Lifshitz theory.

As a first test of the inversion framework, we consider materials whose dielectric response is described solely by a Drude model, which captures the low-frequency electrodynamic behavior of conductive materials using a minimal set of physically interpretable parameters. This simplified case provides a controlled setting in which the relationship between Casimir forces and dielectric response is well understood, allowing us to assess whether broadband optical information can be reliably reconstructed from force–distance data alone. Synthetic permittivity spectra spanning a wide range of plasma frequencies are used to generate corresponding Casimir force curves via Lifshitz theory, and a subset of these data is withheld for validation.

Across this parameter space, the reconstructed permittivity spectra closely reproduce the ground truth for both the real and imaginary components, demonstrating that the inversion accurately captures the broadband response implied by the force measurements. Importantly, the quality of the reconstruction is largely independent of the plasma frequency, indicating that the approach is robust across materials with widely varying characteristic electronic energy scales. These results establish that Casimir force curves contain sufficient information to recover the essential low-frequency optical response of conductive materials.

We evaluated several supervised learning architectures for this inversion task and found that bagging-based ensemble models consistently provided reliable reconstructions of the Drude-only spectra. Because our focus is on the physical content of the inversion rather than algorithmic optimization, we adopt this approach for the remainder of the study. Details of model selection and optimization are provided in the Methods section.

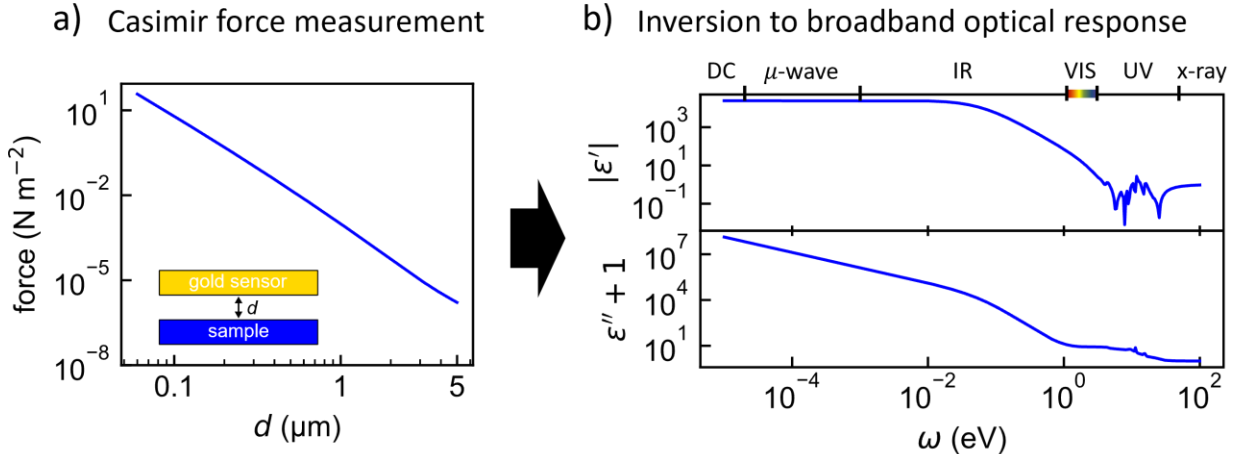


Figure 1 | Conceptual framework for reconstructing broadband dielectric response from Casimir force measurements. **a**, Representative Casimir force as a function of separation between a gold sensing surface and a planar sample with unknown optical properties. Within Lifshitz theory, the force depends on the material's dielectric response across the electromagnetic spectrum. **b**, Schematic illustration of the inversion approach, in which supervised learning models map force–distance curves onto the real and imaginary components of the sample's permittivity over a wide frequency range. This framework exploits the structured dependence of Casimir interactions on broadband quantum electromagnetic fluctuations to recover real-frequency optical properties from force measurements.

Figure 2 demonstrates how Casimir force measurements at different separation distances selectively constrain distinct regions of a material's dielectric response. Using dielectric spectra described by a Drude model, we reconstruct the real and imaginary components of the permittivity from force–distance curves spanning separations from tens of nanometres to several micrometres. For materials with widely varying plasma frequencies, the reconstructed spectra closely reproduce the ground truth across the full frequency range, indicating that the inversion accurately captures the broadband response encoded in the force measurements (Fig. 2a–f).

The sensitivity of the reconstruction to the maximum separation distance provides direct physical insight into how quantum fluctuations sample the electromagnetic spectrum. As the maximum separation d_{\max} included in the force data is reduced, deviations between the reconstructed and true permittivity emerge at low frequencies, while higher-frequency features remain largely unaffected (Fig. 2g,h). This behavior reflects the fact that Casimir interactions at larger separations are dominated by long-wavelength, low-frequency fluctuations, whereas shorter separations weight higher-frequency contributions more strongly.

This separation–frequency correspondence is quantified in Fig. 2j, which shows that the absolute error in the low-frequency limit of the real permittivity decreases systematically with increasing d_{\max} . The observed scaling directly mirrors the known physics of Casimir interactions, in which the contribution of low-frequency electromagnetic modes grows with separation distance. These results demonstrate that access to force measurements at larger separations is essential for accurately reconstructing the low-frequency dielectric response and establish a clear physical mapping between force–distance data and spectral sensitivity.

Together, Fig. 2 reveals that the inversion of Casimir force measurements is not merely a numerical exercise, but reflects a physically structured encoding of broadband optical information by quantum fluctuations. Different portions of the electromagnetic spectrum are accessed by tuning the separation range of the force measurement, providing a direct and intuitive link between Casimir interactions and real-frequency material response.

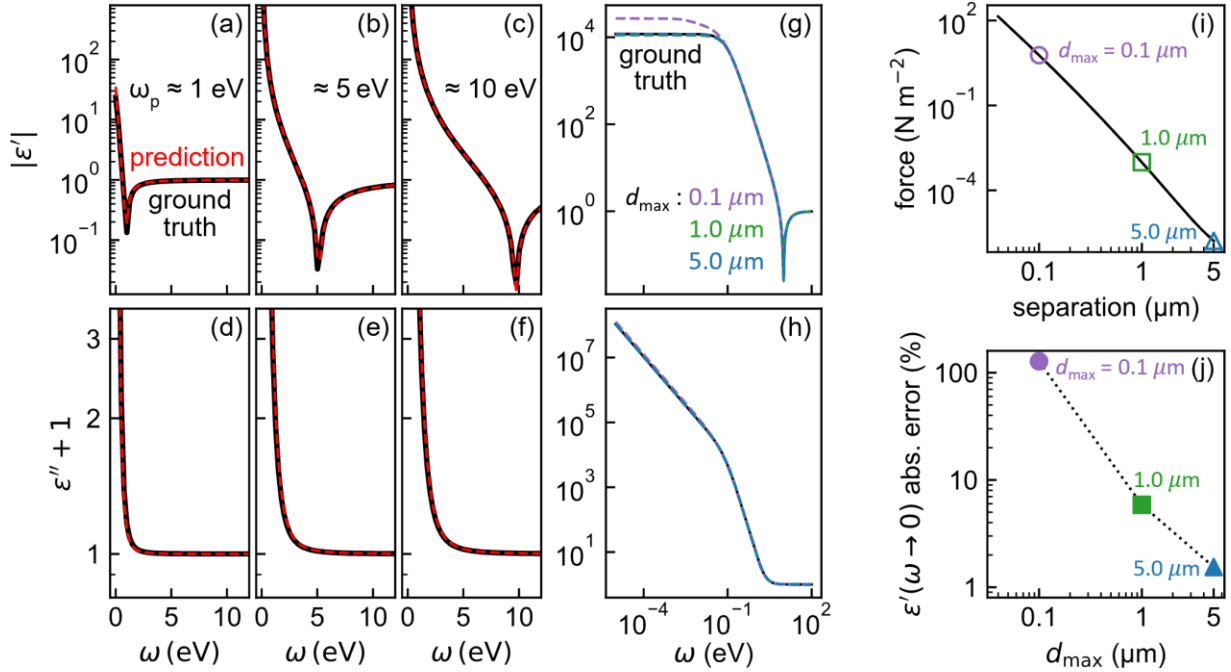


Figure 2 | Separation-dependent reconstruction of dielectric response for Drude-model materials. a–f, Reconstructed real (a–c) and imaginary (d–f) components of the permittivity for synthetic materials with widely varying plasma frequencies, demonstrating accurate recovery of broadband optical response from Casimir force data. g,h, Effect of the maximum separation d_{\max} included in the force–distance data on the reconstructed real (g) and imaginary (h) permittivity. Reducing d_{\max} leads to increased deviations at low frequencies, while higher-frequency response remains comparatively unaffected. i, Representative Casimir force curve indicating the separation ranges used for reconstruction. j, Absolute error in the low-frequency limit of the real permittivity as a function of d_{\max} , showing systematic improvement with increasing maximum separation. These results reveal a direct physical correspondence between measurement separation and spectral sensitivity, reflecting how long-wavelength quantum fluctuations dominate Casimir interactions at large separations.

Figure 3 extends the inversion framework to materials with more complex dielectric response by incorporating Lorentz oscillators in addition to the Drude contribution, enabling resonant behavior at higher frequencies. Using this expanded training set, we reconstruct the permittivity spectra of gold, palladium, and platinum from simulated Casimir force curves generated using experimentally tabulated optical data. This approach allows us to assess how faithfully Casimir force measurements constrain realistic material response beyond the idealized Drude limit.

For all three metals, the reconstructed real and imaginary permittivity closely reproduce the ground truth at low frequencies, where the dielectric response is dominated by free-carrier behavior (Fig. 3d–i). This agreement confirms that Casimir forces robustly encode the low-frequency electrodynamic properties of conductive materials, even in the presence of additional spectral structure. At higher frequencies, the reconstructed spectra capture the presence and approximate

location of resonant features, but deviations from the ground truth become more pronounced, particularly for palladium and platinum in the intermediate frequency range.

These deviations reflect the fact that the experimentally measured optical response of real materials contains features that are not fully described by a limited set of Lorentz oscillators. Because the inversion framework is trained on physically motivated but finite dielectric models, it naturally reproduces spectral behavior that lies within that training space while exhibiting reduced fidelity for features that fall outside it. Importantly, this behavior highlights a physical, rather than algorithmic, limitation: Casimir force measurements constrain broadband optical response through an integral over fluctuations, and fine spectral details that weakly influence the force cannot be uniquely reconstructed without additional physical priors—a well-known difference between the Casimir effect and other optically resonant phenomena.

Figure 3 therefore illustrates both the strengths and boundaries of Casimir-force-based optical reconstruction. While the low-frequency response—which plays a dominant role in Casimir interactions—is recovered with high fidelity, higher-frequency resonant structure is reconstructed more approximately, consistent with its weaker influence on the force. These results underscore the role of Casimir interactions as a broadband, but spectrally weighted, probe of material response.

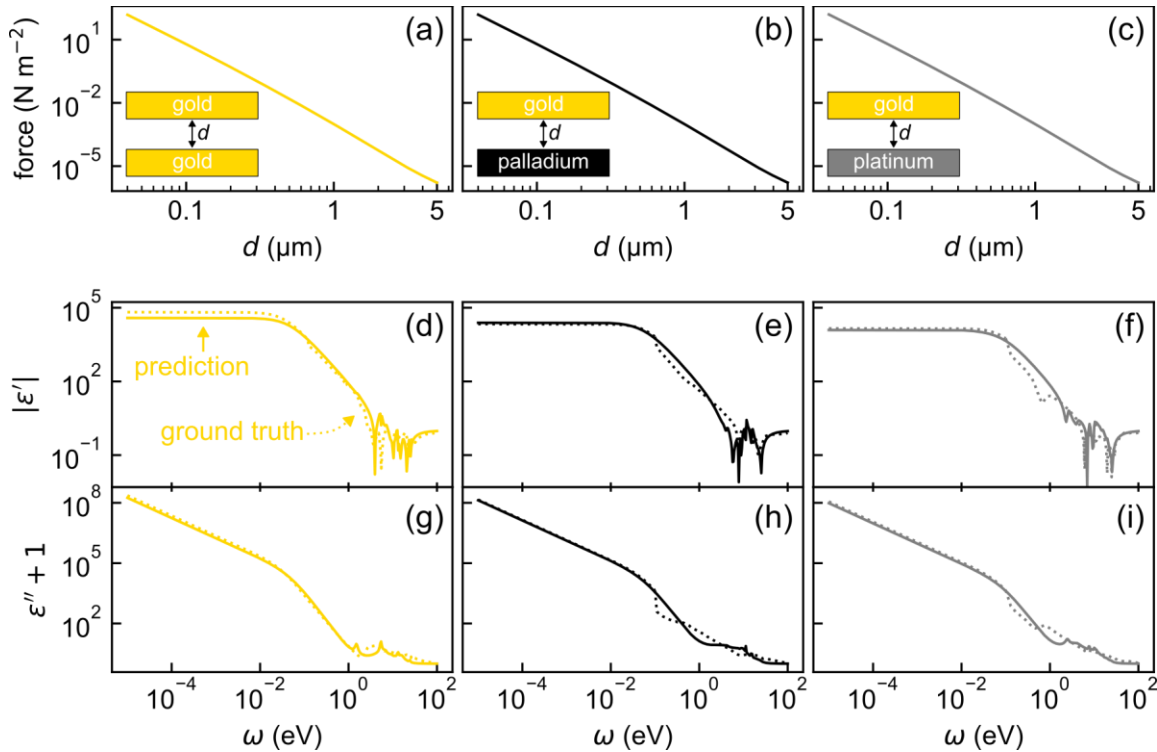


Figure 3 | Reconstruction of realistic dielectric spectra from simulated Casimir force data. **a–c**, Simulated Casimir force curves for gold, palladium, and platinum, generated using experimentally tabulated optical data. **d–f**, Reconstructed real component of the permittivity for each metal, compared with the corresponding ground truth. **g–i**, Reconstructed imaginary component of the permittivity. At low frequencies, where free-carrier response dominates, the reconstructed spectra closely reproduce the ground truth for all materials. At higher frequencies, resonant features are recovered more approximately, reflecting their weaker contribution to the Casimir interaction and the finite physical information encoded in the force. These results illustrate both the robustness and the intrinsic spectral weighting of Casimir-force-based optical reconstruction.

In Figure 4, we apply the inversion framework to experimentally measured Casimir force gradients, providing a stringent test of its performance under realistic measurement conditions. We consider force gradient data obtained using an atomic force microscope between a gold-coated sphere and a gold plate, a geometry commonly employed in precision Casimir measurements [31–34]. To enable direct comparison with the parallel-plate calculations used in training, the measured force gradients are related to the corresponding plate–plate force using the proximity force approximation, which is valid in the limit of large sphere radius relative to separation [35].

To disentangle the effects of experimental noise from the consequences of a restricted separation range, we apply the inversion procedure to both simulated and measured force gradient data spanning the same range of separations (60–400 nm). When applied to simulated force gradients, the reconstructed permittivity closely reproduces the ground truth at low frequencies for both the real and imaginary components (Fig. 4c,d). This result demonstrates that, in principle, force gradient data over this separation range retain sufficient information to constrain the low-frequency optical response.

In contrast, reconstructions based on the experimentally measured force gradients exhibit larger deviations from the ground truth, particularly in the real component of the permittivity. This degradation reflects the sensitivity of the inversion to small levels of noise and systematic error in the force data, which are amplified when reconstructing broadband spectral information. Notably, the imaginary component of the permittivity at the lowest frequencies remains comparatively well constrained, consistent with its dominant contribution to dissipation-related fluctuations. Lastly, the input optical data is derived from measurement of a film that was deposited at the same time that the probing sphere was deposited; however, small differences in the optical properties could arise due to differing surface properties of the probe.

These results highlight two distinct and complementary limitations of Casimir-force-based optical reconstruction. First, access to large separation distances is critical for constraining low-frequency response, as established in Fig. 2; second, experimental noise, error, and uncertainties in the optical properties of the spherical probe place practical limits on the spectral information that can be reliably extracted from measured force data. Figure 4 therefore does not represent a failure of the inversion framework, but rather delineates the experimental conditions under which quantum-fluctuation-based spectroscopy is viable and where further advances in measurement precision or separation control will be required.

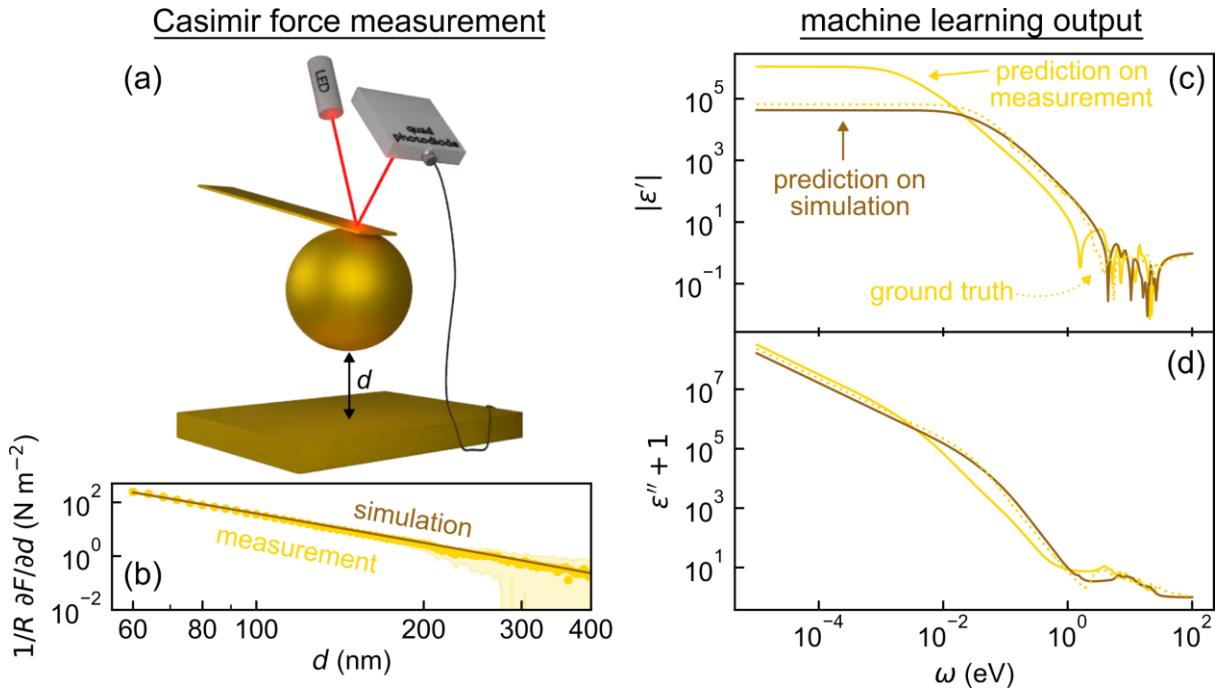


Figure 4 | Application of the inversion framework to experimentally measured Casimir force gradients. a, Schematic of the atomic force microscope geometry used to measure the Casimir force gradient between a gold-coated sphere and a gold plate. b, Measured and simulated Casimir force gradients over the same separation range (60–400 nm). c,d, Reconstructed real (c) and imaginary (d) components of the permittivity of gold obtained from simulated and measured force gradients. Reconstructions based on simulated data closely reproduce the low-frequency optical response, whereas experimental data exhibit larger deviations due to noise, bias, and restricted separation access. These results delineate the experimental conditions under which Casimir-force-based optical reconstruction is viable and highlight the role of measurement precision and separation range in determining spectral sensitivity.

Conclusion

Casimir interactions arise from quantum electromagnetic fluctuations and encode information about a material's dielectric response across the entire electromagnetic spectrum. In this work, we have shown that this global dependence can be exploited to reconstruct a material's broadband optical properties directly from Casimir force measurements. By inverting Lifshitz theory using supervised machine-learning models trained on physically motivated dielectric spectra, we demonstrate that the complex permittivity of a material can be recovered over more than seven orders of magnitude in frequency from a single force–distance curve.

Our results reveal a clear physical structure underlying this inversion. Force measurements at larger separations preferentially constrain the low-frequency dielectric response, whereas shorter separations encode higher-frequency contributions, reflecting how quantum fluctuations of different wavelengths contribute to Casimir interactions. This separation–frequency correspondence establishes Casimir forces as a spectrally weighted probe of material response, rather than an opaque integral over electromagnetic modes. In this sense, quantum fluctuations act as a physically constrained form of broadband spectroscopy, with sensitivity determined by both material properties and measurement geometry.

By extending the approach to realistic dielectric spectra and experimentally measured force gradients, we further delineate the strengths and limitations of Casimir-force-based optical reconstruction. While low-frequency electrodynamic response is robustly constrained, fine spectral features that contribute weakly to the force are reconstructed more approximately, and experimental noise and restricted separation ranges impose practical limits on extractable information. These limitations are not algorithmic in nature, but reflect the fundamental weighting of electromagnetic fluctuations inherent to Casimir interactions.

Together, these findings reposition Casimir forces from a phenomenon that depends on optical properties to a tool for their determination. Beyond enabling an alternative route to broadband optical characterization, this work provides a new perspective on the relationship between quantum fluctuations and real-frequency material response. As experimental capabilities continue to improve, Casimir-force-based spectroscopy may offer access to electromagnetic regimes that are challenging to probe using conventional optical techniques, opening new opportunities at the intersection of quantum electrodynamics, materials science, and precision measurement.

Acknowledgments:

The authors acknowledge financial support from the Defense Advanced Research Projects Agency (DARPA) QUEST Projects Contract No. HR00112090084. C.S. acknowledges support from the National Science Foundation Graduate Research Fellowship Program under Grant No. 2036201. Any opinions, findings, and conclusions or recommendations expressed in this material are those of the author(s) and do not necessarily reflect the views of the National Science Foundation or DARPA.

Author Contributions:

J.N.M. conceived and supervised the project. C.F.S. performed experiments, analysed the resultant data, and performed ML analysis. Both authors discussed and interpreted the data and wrote the manuscript.

Citations

- [1] H. B. G. Casimir, On the Attraction Between Two Perfectly Conducting Plates, *Proc K Ned Akad Wet* **51**, 793 (1948).
- [2] E. M. Lifshitz, The Theory of Molecular Attractive Forces between Solids, *J Exper Theor. Phys USSR* **29**, 94 (1956).
- [3] I. E. Dzyaloshinskii, E. M. Lifshitz, and L. P. Pitaevskii, The General Theory of Van der Waals Forces, *Adv. Phys.* **10**, 165 (1961).
- [4] V. A. Parsegian, *Van Der Waals Forces: A Handbook for Biologists, Chemists, Engineers, and Physicists*, 1st ed. (Cambridge University Press, 2005).
- [5] R. S. Decca, D. López, E. Fischbach, and D. E. Krause, Measurement of the Casimir Force between Dissimilar Metals, *Phys. Rev. Lett.* **91**, 050402 (2003).

- [6] D. Iannuzzi, M. Lisanti, and F. Capasso, Effect of hydrogen-switchable mirrors on the Casimir force, *Proc. Natl. Acad. Sci.* **101**, 4019 (2004).
- [7] G. L. Klimchitskaya, U. Mohideen, and V. M. Mostepanenko, The Casimir force between real materials: Experiment and theory, *Rev. Mod. Phys.* **81**, 1827 (2009).
- [8] J. N. Munday, F. Capasso, and V. A. Parsegian, Measured long-range repulsive Casimir–Lifshitz forces, *Nature* **457**, 170 (2009).
- [9] K. Chen and S. Fan, Nonequilibrium Casimir Force with a Nonzero Chemical Potential for Photons, *Phys. Rev. Lett.* **117**, 267401 (2016).
- [10] R. Zhao, L. Li, S. Yang, W. Bao, Y. Xia, P. Ashby, Y. Wang, and X. Zhang, Stable Casimir equilibria and quantum trapping, *Science* **364**, 984 (2019).
- [11] B. Spreng, C. Shelden, T. Gong, and J. N. Munday, Casimir repulsion with biased semiconductors, *Opt. Quantum* **2**, 266 (2024).
- [12] C. Shelden, B. Spreng, and J. N. Munday, Opportunities and challenges involving repulsive Casimir forces in nanotechnology, *Appl. Phys. Rev.* **11**, 041325 (2024).
- [13] C. Shelden, B. Spreng, J. L. Garrett, T. S. Rahman, J. Kim, and J. N. Munday, Casimir Force Control Enabled by 3D Nanostructures, *Nano Lett.* **25**, 9254 (2025).
- [14] D. A. T. Somers and J. N. Munday, Casimir-Lifshitz Torque Enhancement by Retardation and Intervening Dielectrics, *Phys. Rev. Lett.* **119**, 183001 (2017).
- [15] D. A. T. Somers, J. L. Garrett, K. J. Palm, and J. N. Munday, Measurement of the Casimir torque, *Nature* **564**, 386 (2018).
- [16] P. Thiyam, P. Parashar, K. V. Shajesh, O. I. Malyi, M. Boström, K. A. Milton, I. Brevik, and C. Persson, Distance-Dependent Sign Reversal in the Casimir-Lifshitz Torque, *Phys. Rev. Lett.* **120**, 131601 (2018).
- [17] M. Antezza, H. B. Chan, B. Guizal, V. N. Marachevsky, R. Messina, and M. Wang, Giant Casimir Torque between Rotated Gratings and the $\theta=0$ Anomaly, *Phys. Rev. Lett.* **124**, 013903 (2020).
- [18] B. Spreng, T. Gong, and J. N. Munday, Recent developments on the Casimir torque, *Int. J. Mod. Phys. A* **37**, 2241011 (2022).
- [19] B. Munkhbat, A. Canales, B. Küçüköz, D. G. Baranov, and T. O. Shegai, Tunable self-assembled Casimir microcavities and polaritons, *Nature* **597**, 7875 (2021).
- [20] B. Küçüköz, O. V. Kotov, A. Canales, A. Yu. Polyakov, A. V. Agrawal, T. J. Antosiewicz, and T. O. Shegai, Quantum trapping and rotational self-alignment in triangular Casimir microcavities, *Sci. Adv.* **10**, eadn1825 (2024).
- [21] G. Wang et al., Nanoalignment by critical Casimir torques, *Nat. Commun.* **15**, 5086 (2024).
- [22] M. Hošková, O. V. Kotov, B. Küçüköz, C. J. Murphy, and T. O. Shegai, Casimir self-assembly: A platform for measuring nanoscale surface interactions in liquids, *Proc. Natl. Acad. Sci.* **122**, e2505144122 (2025).
- [23] G. C. Wick, Properties of Bethe-Salpeter Wave Functions, *Phys. Rev.* **96**, 1124 (1954).
- [24] A. Rodriguez, M. Ibanescu, D. Iannuzzi, J. D. Joannopoulos, and S. G. Johnson, Virtual photons in imaginary time: Computing exact Casimir forces via standard numerical electromagnetism techniques, *Phys. Rev. A* **76**, 032106 (2007).
- [25] I. Pirozhenko, A. Lambrecht, and V. B. Svetovoy, Sample dependence of the Casimir force, *New J. Phys.* **8**, 238 (2006).
- [26] V. B. Svetovoy, P. J. van Zwol, G. Palasantzas, and J. Th. M. De Hosson, Optical properties of gold films and the Casimir force, *Phys. Rev. B* **77**, 035439 (2008).

- [27] P. J. van Zwol, G. Palasantzas, and J. Th. M. De Hosson, Influence of dielectric properties on van der Waals/Casimir forces in solid-liquid systems, *Phys. Rev. B* **79**, 195428 (2009).
- [28] A. Formisano and M. Tucci, Machine Learning Approaches for Inverse Problems and Optimal Design in Electromagnetism, *Electronics* **13**, 1167 (2024).
- [29] G. Aarts, K. Fukushima, T. Hatsuda, A. Ipp, S. Shi, L. Wang, and K. Zhou, Physics-driven learning for inverse problems in quantum chromodynamics, *Nat. Rev. Phys.* **1** (2025).
- [30] M. Peng and H. Tang, Information-distilled physics informed deep learning for high order differential inverse problems with extreme discontinuities, *Commun. Eng.* **4**, 150 (2025).
- [31] U. Mohideen and A. Roy, Precision Measurement of the Casimir Force from 0.1 to 0.9 μm , *Phys. Rev. Lett.* **81**, 4549 (1998).
- [32] S. de Man, K. Heeck, R. J. Wijngaarden, and D. Iannuzzi, Halving the Casimir force with Conductive Oxides, *Phys. Rev. Lett.* **103**, 040402 (2009).
- [33] C.-C. Chang, A. A. Banishev, R. Castillo-Garza, G. L. Klimchitskaya, V. M. Mostepanenko, and U. Mohideen, Gradient of the Casimir force between Au surfaces of a sphere and a plate measured using an atomic force microscope in a frequency-shift technique, *Phys. Rev. B* **85**, 165443 (2012).
- [34] J. L. Garrett, D. A. T. Somers, K. Sendgikoski, and J. N. Munday, Sensitivity and accuracy of Casimir force measurements in air, *Phys. Rev. A* **100**, 022508 (2019).
- [35] B. Derjaguin, Theorie des Anhaftens kleiner Teilchen, *Kolloid-Z.* **69**, 155 (1934).
- [36] B. Spreng, sprengjamin/califorcia, (2025).
- [37] G. L. Klimchitskaya, U. Mohideen, and V. M. Mostepanenko, Kramers–Kronig relations for plasma-like permittivities and the Casimir force, *J. Phys. Math. Theor.* **40**, F339 (2007).
- [38] E. D. Palik, *Handbook of Optical Constants of Solids: Volume 2* (Elsevier Science & Technology, San Diego, UNITED STATES, 1991).
- [39] A. D. Rakić, A. B. Djurišić, J. M. Elazar, and M. L. Majewski, Optical properties of metallic films for vertical-cavity optoelectronic devices, *Appl. Opt.* **37**, 5271 (1998).
- [40] N. W. Ashcroft and D. N. Mermin, *Solid State Physics* (Holt-Saunders, 1976).

Methods

1. Casimir force calculations

Casimir forces between planar surfaces are calculated using Lifshitz theory, which expresses the interaction in terms of the frequency-dependent dielectric response of the interacting materials evaluated at imaginary frequencies using the Python library ‘CaLiForcia’ [36]. For each dielectric spectrum considered in this work, the permittivity is analytically continued to imaginary frequencies using a Kramers–Kronig–like relation [37], and the resulting Casimir force is computed by summing the contributions of electromagnetic fluctuations over all Matsubara frequencies.

For simulations involving a gold sensing surface, the dielectric response of gold is taken from experimentally tabulated optical data [38,39] and extrapolated to low frequencies using a Drude model. Temperature effects are included through the Matsubara formalism. Numerical convergence is verified with respect to frequency and wavevector discretization.

2. Synthetic dielectric spectra

To generate physically motivated training data, synthetic dielectric spectra are constructed using combinations of Drude and Lorentz oscillator models. The Drude model captures the low-frequency free-carrier response of conductive materials and is given by [40]:

$$\epsilon(\omega) = 1 - \frac{\omega_p^2}{\omega(\omega + i\gamma)},$$

where ω is the real photon frequency, ω_p is the plasma frequency, and γ is the damping rate. Resonant contributions at higher frequencies are modeled using Lorentz oscillators of the form

$$\epsilon(\omega) = 1 + \sum_{j=1}^N \frac{\Omega_j^2}{\omega_j^2 - \omega^2 - i\gamma_j \omega},$$

where Ω_j , ω_j , and γ_j denote the oscillator strength, resonance angular frequency, and damping coefficient of the j th oscillator, respectively.

Model parameters are randomly sampled over physically reasonable ranges to generate a diverse ensemble of dielectric spectra spanning more than seven orders of magnitude in frequency. This construction ensures that the training data encode realistic electrodynamic behavior while remaining sufficiently general to test the inversion framework.

3. Training data generation

For each synthetic dielectric spectrum, the corresponding Casimir force is calculated over a discrete set of separation distances ranging from 40 nm to 5 μm , unless otherwise stated. Force–distance curves are sampled at uniformly spaced separations, providing between several tens and one hundred force values per spectrum, depending on the separation range considered.

The real and imaginary components of the dielectric function are evaluated on a frequency grid spanning more than seven orders of magnitude in energy, from the far-infrared to the ultraviolet. These discretized spectra serve as the target outputs for supervised learning, while the corresponding force–distance curves serve as the input features.

In total, several thousand synthetic dielectric spectra and their associated Casimir force curves are generated and randomly divided into training and validation sets. Validation data are withheld entirely from model training and are used exclusively to evaluate reconstruction accuracy, ensuring that reported results reflect genuine inversion capability rather than memorization of the training data.

4. Machine-learning inversion

The inversion of Casimir force measurements into dielectric spectra is formulated as a supervised regression problem. We evaluated several supervised learning architectures, including decision trees, gradient-boosted trees, random forests, and deep neural networks, using synthetic force–distance data generated from Lifshitz theory (Supplementary Fig. S1). Across this parameter space, a random forest method consistently provided reliable and robust reconstructions and is therefore used for all results presented in the main text.

Model hyperparameters are optimized using grid search with the coefficient of determination as the scoring metric, and performance is evaluated using withheld validation data, where applicable. Hyperparameter optimization is performed independently for multiple training data sets spanning different dielectric model complexities (Supplementary Figs. S2–S4). To reduce overfitting and improve generalization, each prediction is obtained by averaging over multiple independently trained ensemble members.

Because all training data are generated using Lifshitz theory with physically motivated dielectric models, the learned inversion is intrinsically constrained by electrodynamics. The machine-learning framework therefore serves to approximate the nontrivial inverse mapping implied by the theory, rather than introducing an unconstrained, purely data-driven model.

5. Experimental force gradient measurements

We measure the Casimir force gradient between a gold-coated spherical AFM probe and a gold-coated Si plate in ambient conditions using an amplitude-modulated measurement scheme described in Ref. [34]. We fabricate the spherical AFM probe using a tipless AFM cantilever (Bruker, MLCT-O10) and hollow glass sphere (Trelleborg, SI-100), and coat both the AFM probe and a Si plate with 100 nm of gold using an electron beam evaporator (CHA). The coated sphere has a radius of $R = 37.69 \mu\text{m}$, which we determined from a scanning electron micrograph.

Measured force gradient data are binned to reduce noise, and the resulting force–distance curves are used as input to the inversion framework without additional fitting or preprocessing. Simulated force gradients over the same separation range are used to isolate the effects of experimental noise and bias from limitations imposed by restricted separation access.